DALTON
FULL PAPER

Complexed bridging ligands: oxorhenium(v) compounds with mono-coordinated pyrazine or pyrimidine as possible building blocks for the construction of polynuclear architectures †

Elisabetta Iengo, Ennio Zangrando, Stefano Mestroni, Giovanna Fronzoni, Mauro Stener and Enzo Alessio *

Dipartimento di Scienze Chimiche, Università di Trieste, Via L. Giorgieri 1, 34127 Trieste, Italy. Fax: 040 6763903; E-mail: alessi@univ.trieste.it

Received 20th November 2000, Accepted 28th February 2001
First published as an Advance Article on the web 29th March 2001

The reactivity of oxorhenium(v) precursors with simple diaza ligands such as pyrazine (pyz) and pyrimidine (pym) was investigated. Treatment of $ReOCl_3(Me_2S)(OPPh_3)$ or $ReO(OEt)Cl_2(PPh_3)_2$ with an excess of pyz or pym under a range of different conditions yielded a series of oxo- and dioxo-rhenium(v) compounds with one or more terminally coordinated diaza ligands, namely the dinuclear species $Re_2O_3Cl_4(pyz)_4$ **1** and $Re_2O_3Cl_4(pym)_4$ **2**, and the mononuclear complexes *trans*,*trans*,*trans*-$ReO(OEt)Cl_2(pyz)_2$ **3**, *trans*,*trans*,*trans*-$ReO(OEt)Cl_2(pym)_2$ **4**, *trans*,*trans*,*trans*-$ReO(OEt)Cl_2(pyz)(PPh_3)$ **5**, and [*trans*-$ReO_2(pyz)_4$][PF_6] **7**. The new compounds were characterized in solution and in the solid state by common spectroscopic techniques; the crystal structures of **1**, **3**, **5**, and **7** were also determined. The dinuclear species **1** presents a nearly linear O=Re–O–Re=O group and each Re atom brings two *cis* chlorides and two mono-coordinated pyrazine units. Crystals of the dioxo species **7** contain one $NaPF_6$ and two H_2O molecules of crystallization; the four pyrazine bases terminally bound to Re interact also with Na, forming slightly distorted square cavities (side length *ca*. 7.4 Å), with Na and Re alternating in the corners. Density functional calculations of the excitation spectra of **3** and **4** were also performed with the aim of investigating in more detail the influence of the nature of the nitrogen ligand on the experimental visible spectra. A preliminary investigation of the reactivity of compound **3** towards coordination compounds and metalloporphyrins was also made. Treatment of **3** with a slight excess of the ruthenium(ii) complex *cis*,*fac*-$RuCl_2(Me_2SO)_3(CO)$ yielded the linear trinuclear species [{*trans*,*trans*,*trans*-$ReO(OEt)Cl_2$}(μ-pyz)$_2${*cis*,*cis*,*cis*-$RuCl_2(Me_2SO\text{-}S)_2(CO)$}$_2$], in which both ends of the rhenium complex are bound to a ruthenium coordination compound. Similarly, treatment of **3** with an excess of [Ru(TPP)(CO)(EtOH)] (TPP = tetraphenylporphyrinate) led to the symmetrical trinuclear species [{*trans*,*trans*,*trans*-$ReO(OEt)Cl_2$}(μ-pyz)$_2${Ru(TPP)(CO)}$_2$], consisting of two face-to-face ruthenium porphyrins axially connected through a coordination compound; the corresponding canted trinuclear compound [{*trans*,*trans*,*trans*-$ReO(OEt)Cl_2$}(μ-pym)$_2${Ru(TPP)(CO)}$_2$] was similarly obtained from **4**. Thus the new oxorhenium(v) species can be considered as potentially useful basic building blocks for the self-assembly of polynuclear architectures.

Introduction

Supramolecular chemistry is at the forefront of modern chemistry and recent years have witnessed a growing number of supramolecular systems which incorporate metal ions as assembling and organizing centers.[1] In fact, it is now widely recognized that the formation of metal–ligand dative bonds is an attractive alternative to covalent synthesis for the construction of stable nanoscale assemblies. Moreover, inorganic architectures that incorporate metal ions as integral structure-generating units are expected to exhibit novel and interesting physicochemical properties such as optical, magnetic, electrochemical, and catalytic functions.

Most of the metal-mediated supramolecular assemblies reported to date have been obtained by treatment of metal complexes bearing good leaving groups in a well defined geometry (acidic building blocks) with di- or poly-dentate organic ligands having appropriate donor atoms (mainly nitrogen) in a desired spatial orientation (basic building blocks). However, there is an increasing number of reports describing the use of complexed bridging ligands for the controlled assembly of multi-metal supramolecular adducts.[2] This modular synthetic approach offers, in principle, a much higher degree of complexity and of potential future developments compared to that involving merely organic basic units. In particular, the possibility of controlling parameters such as coordination geometry and charge density of each individual metal subunit may allow one to vary physical dimensions as well as shape, charge distribution, and solubility of the polynuclear supramolecular architecture.

Within this framework, one of our current goals is the development of a set of coordination compounds of various geometries bearing mono-coordinated bridging ligands to be used as basic building blocks in the construction of multi-metal supramolecular assemblies. Such compounds must fulfill the following requirements: the metal–terminus bond of each complexed ligand has to be stable and preferably inert and the peripheral uncoordinated terminus must be capable of further binding to metal centers. Since the primary focus of our systematic approach is on the geometry of the complexes, we are investigating different metals.

In this respect, oxorhenium(v) species with monodentate diaza ligands seemed good candidates. Since the pioneering work of Johnson *et al.*,[3,4] the reactivity of common oxorhenium(v) precursors towards simple aromatic N-donor

† Electronic supplementary information (ESI) available: packing diagram of **7**, ^{1}H NMR spectrum of **5**, contour plots of **3**, reaction path of **3**, complexation induced shifts of **14** and **15**. See http://www.rsc.org/suppdata/dt/b0/b009295i/

 DOI: 10.1039/b009295i

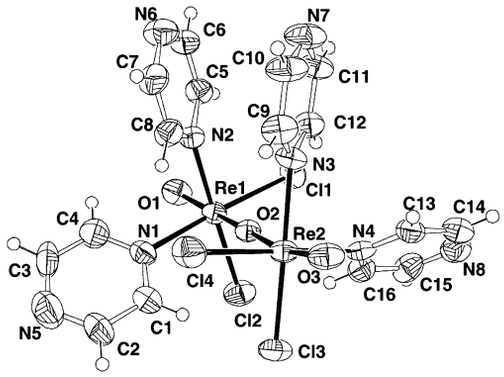

Fig. 1 ORTEP[9] drawing (50% probability for thermal ellipsoids) of the compound $Re_2O_3Cl_4(pyz)_4$ **1**. Selected bond lengths (Å) and angles (°): Re(1)–O(1) 1.706(7); Re(1)–O(2) 1.921(5); Re(1)–N(1) 2.161(8); Re(1)–N(2) 2.175(7); Re(1)–Cl(1) 2.377(2); Re(1)–Cl(2) 2.348(2); Re(2)–O(3) 1.688(7); Re(2)–O(2) 1.926(5); Re(2)–N(4) 2.131(8); Re(2)–N(3) 2.165(7); Re(2)–Cl(3) 2.350(2); Re(2)–Cl(4) 2.381(3); O(1)–Re(1)–O(2) 168.0(3); N(2)–Re(1)–Cl(2) 175.5(2); N(1)–Re(1)–Cl(1) 175.6(2); O(3)–Re(2)–O(2) 167.3(3); N(3)–Re(2)–Cl(3) 175.9(2); N(4)–Re(2)–Cl(4) 176.4(2); Re(1)–O(2)–Re(2) 179.0(3).

ligands, such as pyridine (py) and 3,5-lutidine (3,5-dimethylpyridine) (3,5-lut), has been investigated by a number of authors, including ourselves, over the last 35 years. In particular Lock and Turner prepared and characterized, also by X-ray crystallography, three oxorhenium(v)–py compounds, namely the dinuclear species $Re_2O_3Cl_4(py)_4$,[5] and the monomers *trans*,*trans*,*trans*-$ReO(OEt)Cl_2(py)_2$[6] and [*trans*-$ReO_2(py)_4$]Cl.[7] We therefore decided to investigate the chemistry of oxorhenium(v) species with simple heterocyclic nitrogen bridging ligands such as pyrazine (pyz) and pyrimidine (pym). Pyrazine is a linear bridging ligand and allows coordination of two metal centers at 180° from each other, while pyrimidine might afford coordination of two metal centers at 120°.

Results and discussion

Synthesis and solid state structures

Treatment of $ReOCl_3(Me_2S)(OPPh_3)$ with an excess of pyrazine (pyz) in acetone (Scheme 1) yielded an emerald green solution

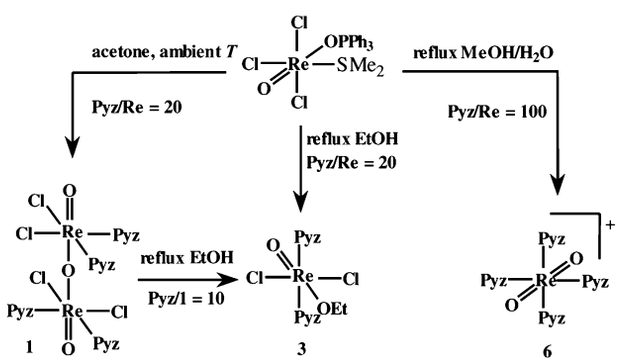

Scheme 1 Reactivity pathways of the oxorhenium(v) precursor $ReOCl_3(Me_2S)(OPPh_3)$ with pyrazine leading to compounds $Re_2O_3Cl_4(pyz)_4$ **1**, *trans*,*trans*,*trans*-$ReO(OEt)Cl_2(pyz)_2$ **3**, and [*trans*-$ReO_2(pyz)_4$]Cl **6**.

from which crystals of the dinuclear compound $Re_2O_3Cl_4(pyz)_4$ **1** formed upon concentration. The corresponding pyrimidine (pym) dimer $Re_2O_3Cl_4(pym)_4$ **2** was obtained analogously. This procedure is similar to that reported by us for the dinuclear oxorhenium(v) species $Re_2O_3Cl_4(3,5\text{-lut})_4$ and $Re_2O_3Cl_4(Me_3Bzm)_4$ (Me_3Bzm = 1,5,6-trimethylbenzimidazole).[8]

A perspective drawing of the dinuclear complex **1** is given in Fig. 1. The structure presents a nearly linear O=Re–O–Re=O group with the metals in a pseudo-octahedral coordination environment, slightly displaced (about 0.08 Å) from the N_2Cl_2 mean plane towards the terminal oxo ligand. Each Re atom brings two *cis* chlorides and two mono-coordinate pyrazine units.‡ The two halves of the dimer are rotated about the fragment Re–O–Re away from an eclipsed conformation; thus one nitrogen ligand on each Re atom is stacked with the corresponding one on the other Re (pyz^s for "stacked"), while the other is designated as pyz^t for "terminal"; in **1** the two stacking pyrazines have the shortest distance of 3.54(1) Å between N(2) and N(3). If the intermetallic vector is regarded as a bond, the pseudo "torsion angles" N(2)–Re(1)···Re(2)–N(3) and N(1)–Re(1)···Re(2)–N(4) are −26.1(3) and 152.4(3)°, respectively, and the pyrazine mean planes, at each metal, make dihedral angles of 64.9(4) (N(1)/N(2)) and 63.7(3)° (N(3)/N(4)). The overall molecular structure closely resembles those found for analogous complexes containing four equal planar N-donor ligands, such as pyridine,[5] Me_3Bzm,[8] and 3,5-dimethylpyrazole[12] or two different planar N-donor ligands (py/Me_3Bzm or 3,5-lut/Me_3Bzm) on each Re atom.[13] The coordination bond distances and angles compare well within their e.s.d.s with those detected in the rhenium(v) compounds mentioned above.

It has been reported that a suspension of the dimer $Re_2O_3Cl_4(py)_4$ is slowly transformed into the monomeric species *trans*,*trans*,*trans*-$ReO(OEt)Cl_2(py)_2$ by prolonged heating in refluxing ethanol.[4] In the case of $Re_2O_3Cl_4(pyz)_4$ and $Re_2O_3Cl_4(pym)_4$ this procedure rapidly led to decomposition of the dimers, yielding only dark, very unsoluble precipitates. Transformation of dimers **1** and **2** into the monomers *trans*,*trans*,*trans*-$ReO(OEt)Cl_2(pyz)_2$ **3** and *trans*,*trans*,*trans*-$ReO(OEt)Cl_2(pym)_2$ **4**, respectively, occurred only when reflux was performed in the presence of an excess (10 : 1) of the corresponding nitrogen ligand (Scheme 1). The reactions are accompanied by dramatic color changes: both **1** and **2** are emerald-green, while **3** is blue-green and the corresponding pyrimidine complex **4** is light violet. Compounds **3** and **4** were more straightforwardly obtained in high yield by treatment of $ReOCl_3(Me_2S)(OPPh_3)$ with an excess of the diaza ligand in refluxing ethanol (Scheme 1).

Compound **4** was obtained also by treatment of $ReO(OEt)Cl_2(PPh_3)_2$ (another widely used rhenium(v) precursor, from which also $ReOCl_3(Me_2S)(OPPh_3)$ is synthesized) with an excess of pyrimidine in refluxing ethanol. However, the same reaction performed with pyrazine led to substitution of only one PPh_3 molecule and *trans*,*trans*,*trans*-$ReO(OEt)Cl_2(pyz)(PPh_3)$ **5** was isolated in good yield.

Compounds **3** and **5** consist of discrete monomers (Figs. 2 and 3, respectively) in which the rhenium center has a slightly distorted octahedral coordination geometry. In both complexes the Re–Cl, Re=O, and Re–O bond distances are similar (within their experimental errors) and agree well with values determined previously in similar compounds, although the structure of **3** is less accurate. The pyrazine rings in **3** are almost coplanar, with the pseudo torsion angle C(1)–N(1)···N(3)–C(8) of 4(2)°, and form angles of 58.6(5) and 55.9(6)° with the best plane through N2Cl2. This conformation is similar to that found in the strictly analogous compound *trans*,*trans*,*trans*-$ReO(OEt)Cl_2(py)_2$.[6] The alignment of the ring planes seems to be unrelated to packing factors; in fact, a search in the Cambridge Crystallographic Database[14] evidenced a variety of rhenium complexes containing imidazoles or pyridines *trans* to each other and having the same conformation, regardless of the nature of the counter anions and of different lattice solvents present.

In compound **5** the Re–N and Re–P bond lengths of 2.219(5) and of 2.432(1) Å, respectively, compare well with those of 2.185(7) and 2.463(2) Å found in the *trans*,*trans*,*trans*-

‡ The structural characterizations of two all-*trans* dinuclear species, $Re_2O_3Cl_4(1\text{-Meim})_4$ (1-Meim = 1-methylimidazole),[10] and $Re_2O_3Cl_4(py)_4$,[11] have been reported.

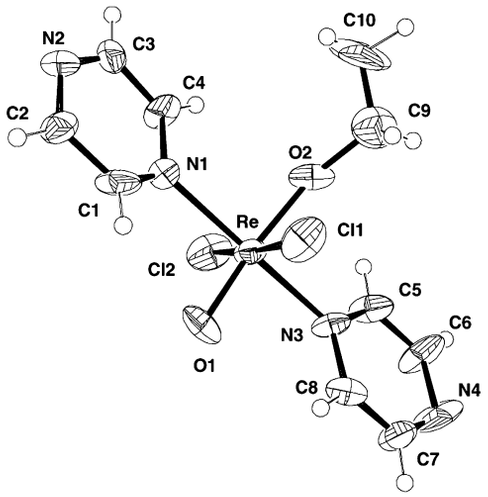

Fig. 2 ORTEP drawing (50% probability for thermal ellipsoids) of the compound *trans*,*trans*,*trans*-$ReO(OEt)Cl_2(pyz)_2$ **3**. Selected bond lengths (Å) and angles (°): Re–O(1) 1.672(14); Re–O(2) 1.837(14); Re–N(1) 2.152(16); Re–N(3) 2.103(16); Re–Cl(1) 2.423(6); Re–Cl(2) 2.357(6); O(1)–Re–O(2) 171.0(6); N(1)–Re–N(3) 177.1(7); Cl(1)–Re–Cl(2) 174.5(2).

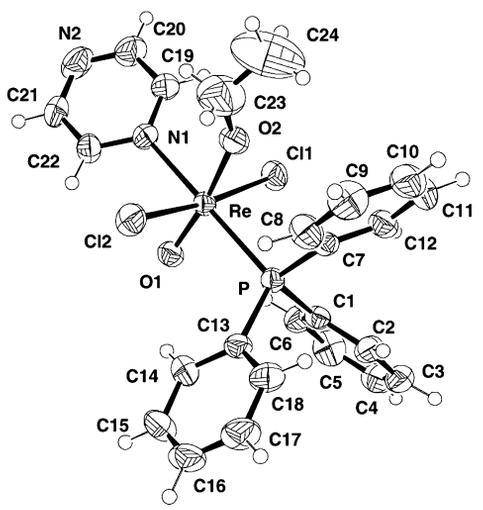

Fig. 3 ORTEP drawing (50% probability for thermal ellipsoids) of the compound *trans*,*trans*,*trans*-$ReO(OEt)Cl_2(pyz)(PPh_3)$ **5**. Selected bond lengths (Å) and angles (°): Re–O(1) 1.697(4); Re–O(2) 1.867(5); Re–N(1) 2.219(5); Re–P 2.432(1); Re–Cl(1) 2.394(2); Re–Cl(2) 2.410(2); O(1)–Re–O(2) 172.3(2); Cl(1)–Re–Cl(2) 172.06(6); N(1)–Re–P 179.28(13).

$ReO(OEt)Cl_2(PPh_3)$(7-azaindole) complex.[15] The former distance is affected by the *trans* influence of the phosphine and is therefore longer than the Re–N distances detected in **3** (2.10(2), and 2.15(2) Å) and in $ReO(OEt)Cl_2(py)_2$ (2.144(7) and 2.132(7) Å),[6] where the N-bases are *trans* to each other. The values of the bond angle at the oxygen atom in the ethoxy group (150(1)° in **3** and 146.1(6)° in **5**) are close to those detected in other complexes containing the same ligand. Some authors suggested that a partial multiple character for the Re–O bond may account for this unusual large value, although steric requirements are not to be excluded.[6,15]

Treatment of *mer*-$ReCl_3O(Me_2S)(OPPh_3)$ with a large excess of pyz in refluxing methanol/water led to the isolation of the dioxo complex [*trans*-$ReO_2(pyz)_4$]Cl **6** (Scheme 1); a similar procedure, using $ReOCl_3(PPh_3)_2$ as precursor, has been reported for the synthesis of the py analog.[3] Compound **6** however contains four HCl molecules of crystallization, which very likely protonate the uncoordinated terminus of each pyz ligand. Crystals suitable for X-ray investigation were obtained for the corresponding PF_6^- salt, [*trans*-$ReO_2(pyz)_4$][PF_6] **7**; the crystals

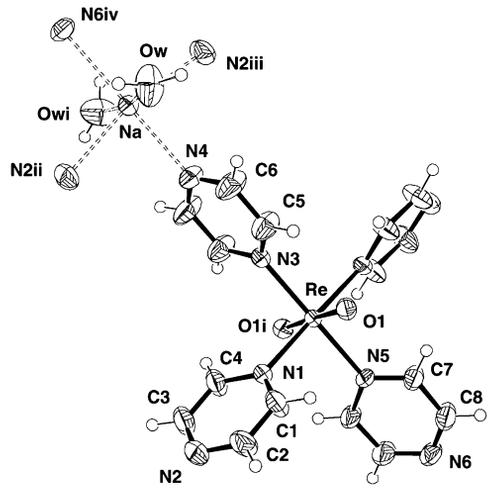

Fig. 4 ORTEP drawing (50% probability for thermal ellipsoids) of the coordination cores of Re and Na in compound [*trans*-$ReO_2(pyz)_4$][PF_6]·$NaPF_6$·$2H_2O$ **7**. The metals and the nitrogen atoms N(4–6) are located on crystallographic twofold axes. Selected bond lengths (Å) and angles (°): Re–O(1) 1.755(4); Re–N(1) 2.141(4); Re–N(3) 2.138(6); Re–N(5) 2.145(6); O(1)–Re–$O(1)^i$ 178.0(2); N(1)–Re–$N(1)^i$ 179.1(2); N(3)–Re–N(5) 180.0; Na–Ow 2.336(4); Na–$N(2)^{ii}$ 2.482(5); Na–N(4) 2.439(7); Na–$N(6)^{iv}$ 2.518(7); Ow–Na–Ow^i 170.3(3); $N(2)^{ii}$–Na–$N(2)^{iii}$ 167.1(3); N(4)–Na–$N(6)^{iv}$ 180.0. Symmetry transformations: i) $-x+\frac{3}{2}, y, -z+\frac{3}{2}$; ii $-x+2, -y+1, -z+1$; iii $x-\frac{1}{2}, -y+1, z+\frac{1}{2}$; iv $x, y-1, z$.

contain one $NaPF_6$ and two H_2O molecules of crystallization. The coordination motif of compound **7** is shown in Fig. 4. The metals present a slightly distorted octahedral environment and are located together with the pyrazine nitrogen atoms N(3–6) on a crystallographic twofold axis, that relates the N(1) pyrazines, the oxo ligands O(1), as well the water molecules coordinating the sodium ion. The Re=O distance of 1.755(4) Å and the Re–N distances (from 2.138(6) to 2.145(6) Å) lie in the range usually detected in other *trans*-dioxo $[ReO_2L_4]^+$ cations (where L = py[7] or imidazole[16]); the bases in *trans* position are tilted with respect to each other, with pseudo torsion angles C(5)–N(3)···N(5)–C(7) and C(1)–N(1)···N(1′)–C(4′) of 54.7(5) and 25.5(5)°, respectively. Each sodium ion interacts with the uncoordinated terminus of four pyrazine ligands at distances in the range 2.439(7)–2.518(7) Å, and with two oxygens from water molecules at 2.336(4) Å. The difunctional pyrazine bases, coordinating both the rhenium and sodium ions, form slightly distorted square cavities (side length *ca*. 7.4 Å), with Re and Na alternating at the corners (angle Na–Re–Na 86.6°, Re–Na–Re 93.4°) and the pyrazine rings at the sides. These square boxes are piled to form "walls" (Fig. 5) that sandwich the PF_6^- anions (see ESI).

The solid state infrared spectra of compounds **1**–**7** are characterized by a sharp absorption at about 1590 cm^{-1}, which is typical for mono-coordinated diaza ligands ("breathing mode"),[17] and by the Re=O stretching vibration at about 970 cm^{-1} (**1**–**5**); the dioxo species **6** and **7** exhibit the asymmetric O=Re=O stretching vibration at about 815 cm^{-1}.

Solution studies

Compounds **1**–**7** have been characterized in solution by UV-vis and NMR spectroscopy. Dinuclear compounds $Re_2O_3Cl_4(pyz)_2$ **1** and $Re_2O_3Cl_4(pym)_2$ **2** are well soluble but unstable in DMSO, acetonitrile, and nitromethane; in these solvents the initially emerald-green solutions turned colorless within a few hours at ambient temperature. Time-driven NMR spectra of **1** in DMSO-d_6 evidenced that the two resonances of the starting complex were rapidly replaced by that of uncoordinated pyrazine; no intermediate was detected.

The dimers are also moderately soluble, and stable, in acetone and dichloromethane. In previous studies we invest-

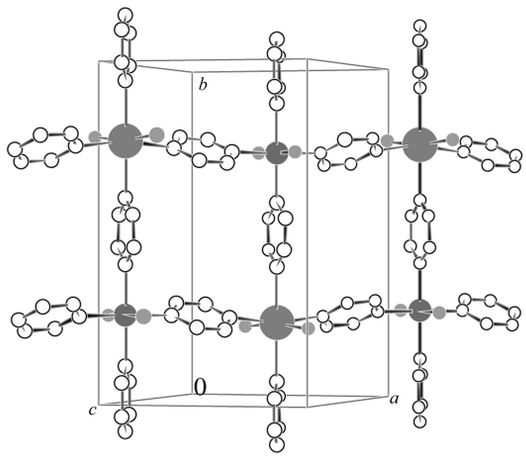

Fig. 5 Packing diagram of [*trans*-$ReO_2(pyz)_4$][PF_6]·$NaPF_6$·$2H_2O$ **7**: side view of the unit cell with the layered structure made up by the metals and pyrazine bases (sodium bigger ion, PF_6^- anions omitted for clarity).

igated the solution conformations of several oxorhenium(v) dinuclear complexes of general formula $Re_2O_3Cl_4(L1)_2(L2)_2$, in which the two *cis* N donor ligands L1 and L2 on each Re atom may be either equal or different from one another.[8,13] Using 2-D exchange nuclear Overhauser effect spectroscopy (NOESY/EXSY), we found that such dimers have a complicated dynamic behavior in solution that involves rotation about the Re–O–Re bond system and also about the Re–N bonds. These motions exchange the stacking ligands with the terminal ones in a pairwise fashion. The ^{1}H NMR spectra of both **1** and **2** in CD_2Cl_2 at 20 °C show only one set of resonances; in **1** the chemically, but not magnetically, equivalent pairs of protons (H2 and H6; H3 and H5, Chart 1) have a single resonance. The small number of NMR resonances observed for **1** and **2** at ambient temperature suggests that both dinuclear complexes, like the similar C_2-symmetric $Re_2O_3Cl_4(Me_3Bzm)_4$ and $Re_2O_3Cl_4(3,5\text{-lut})_4$ compounds,[8] are fluxional molecules; in particular, exchange of terminal and stacking positions is fast and the heterocyclic ligands are in rapid rotation about the Re–N bond on the NMR timescale. All the signals of $Re_2O_3Cl_4(pyz)_2$ **1** broaden considerably below −40 °C and are nearly undetectable at −100 °C, indicating that, unlike in the similar compound $Re_2O_3Cl_4(3,5\text{-lut})_4$,[8] the dynamic motions have not reached the slow limit even at the lowest temperature.

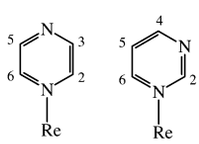

Chart 1 Schematic structures of pyrazine and pyrimidine with numbering schemes when coordinated to rhenium.

Both *trans*,*trans*,*trans*-$ReO(OEt)Cl_2(pyz)_2$ **3** and *trans*,*trans*,*trans*-$ReO(OEt)Cl_2(pym)_2$ **4** are well soluble in chloroform and their solutions are stable. Replacement of pyrazine with pyrimidine induces a remakable change in color of the complex solution, from blue-green (**3**) to light violet (**4**). The visible spectra of both complexes (Fig. 6) are characterized by a very broad (*ca*. 200 nm) and weak absorption band at about 580 nm; the color is fine tuned by a sharper and more intense band in the blue region of the spectrum, whose position depends strongly on the nature of the ligand (see below): 415 nm for pyz *vs*. 386 nm for pym (to be compared with 344 nm for the corresponding py compound, *trans*,*trans*,*trans*-$ReO(OEt)Cl_2(py)_2$ **8**, which has a brilliant blue color). In the ^{1}H NMR spectrum of **3** the two equivalent mono-coordinated pyz ligands give two equally intense multiplets for H2,6 (δ 8.78) and H3,5 (δ 8.95) (Chart 1), both slightly downfield compared to the singlet of unbound

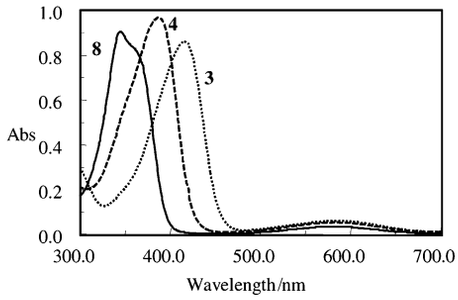

Fig. 6 Electronic absorption spectra ($CHCl_3$, optically matched solutions) for *trans*,*trans*,*trans*-$ReO(OEt)Cl_2(L)_2$ complexes (L = pyz (**3**, ·····), pym (**4**, — — —), py (**8**, ———)).

pyrazine (δ 8.59). A positive NOE effect between the upfield pyz resonance of **3** and the OCH_2 quartet of the *cis* ethoxy group allowed us to assign the δ 8.78 multiplet to the protons in 2,6 positions (from the solid state structure, the calculated distance between one H2,6 and one OCH_2 proton is indeed quite short, 2.9 Å, and compatible with the occurrence of an Overhauser effect). Similarly, in the NMR spectrum of **4** the OCH_2 resonance has positive NOE effects with both the H2 singlet and the most downfield doublet, which was thus attributed to H6 (Chart 1). In both **3** and **4** the resonances for the ethoxide group (a quartet at about δ 3.8 and the corresponding triplet at about δ 1.0) are very similar to those reported for the corresponding py complex.[6]

The $CDCl_3$ ^{1}H NMR spectrum of *trans*,*trans*,*trans*-$ReO(OEt)Cl_2(pyz)(PPh_3)$ **5** at ambient temperature is rather complicated due to partial decomposition of the complex; the number of resonances is thus much higher than expected. For example, there are four sets of resonances for the OCH_2CH_3 moiety, including those of unbound EtOH that account for *ca*. 45% of the total. The region of the phenyl resonances is complicated by the overlap of several multiplets; proton resonances in the region of pyrazine are rather broad, suggesting that at ambient temperature exchange processes involving this ligand occur at an intermediate-to-slow rate on the NMR timescale. At −20 °C such signals become sharp and the resonances for unbound pyrazine and for the bis-pyrazine compound **3** become clearly detectable (see ESI). At this temperature, integration indicates that the main set of resonances (not considering those of unbound ligands) belongs to a species that has bound pyrazine (terminal), ethoxide, and PPh_3 in a 1 : 1 : 1 ratio and was thus safely attributed to **5**. The ethoxide resonances in **5** are upfield shifted compared to those of **3**, presumably because of the shielding effect of the phenyl rings of PPh_3 (an even larger upfield shift was observed in the bis phosphine analog *trans*,*trans*,*trans*-$ReO(OEt)I_2(PPh_3)_2$[18]). Other minor species, one of which contains the ethoxy ligand and accounts for *ca*. 5% of the total, were not identified. The ^{31}P-{^{1}H} NMR spectrum shows five singlets between δ −4.3 and −29.2, including that for uncoordinated PPh_3 at δ −5.3; the most intense resonance at δ −5.5 was attributed to **5**. In conclusion, upon dissolution of **5** in $CDCl_3$ a number of dissociation/coordination equilibria involving pyz, PPh_3 and EtOH are rapidly established; according to integration, the amounts of **3** and **5** in the equilibrium mixture (at −20 °C) correspond to *ca*. 10 and 40% of the total, respectively.

The D_2O NMR spectrum of [*trans*-$ReO_2(pyz)_4$][PF_6] **7** is very simple, as expected for such an highly symmetrical complex, and consists of two equally intense multiplets at δ 9.11 and 8.77 for the four equivalent pyz ligands. Comparison with the spectrum of **3** suggests that the upfield multiplet should be attributed to protons closest to the coordinated nitrogen atoms, *i.e.* to H2,6.

Theoretical excitation spectra

The trend observed in the visible excitation spectra of

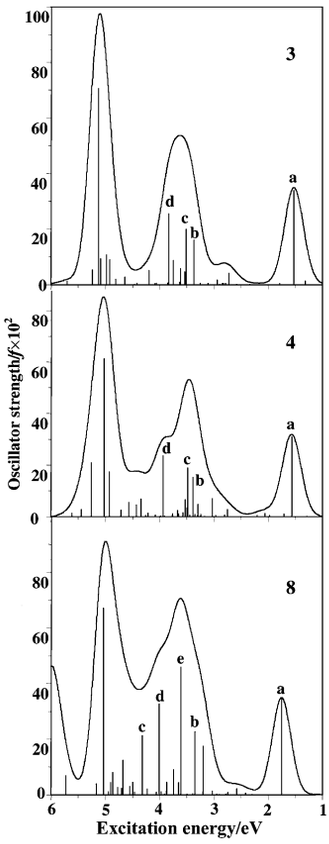

Fig. 7 Calculated valence excitation spectra for *trans*,*trans*,*trans*-$ReO(OEt)Cl_2(L)_2$ complexes (L = pyz (**3**, top), pym (**4**, medium) or py (**8**, bottom)). Lines are convoluted with gaussians of 0.4 eV FWHM (full width of half maximum).

trans,*trans*,*trans*-$ReO(OEt)Cl_2(L)_2$ complexes (L = pyz (**3**), pym (**4**) or py (**8**), see above) suggested a dependency on the nature of the nitrogen ligand L (Fig. 6). With the aim of investigating in more detail such a hypothesis we performed density functional calculations of the spectral properties of compounds **3**, **4**, and **8**. The calculated excitation spectra are shown in Fig. 7. Three definite structures are clearly apparent in all spectra: a low energy band at about 1.6 eV (*ca*. 770 nm) well separated from a second intense and quite broad structure that extends from *ca*. 3 up to about 4.5 eV (*ca*. 400–270 nm) and a last higher energy band at *ca*. 5 eV. For comparison with the visible experimental spectra we consider only the first two low energy calculated structures; the third band falls well in the UV energy region and is reported in the theoretical spectra only for completeness.§

The low energy feature in each calculated spectrum is contributed by a single transition (labelled **a** in Fig. 7), whose energy and oscillator strength value are practically constant along the series, and corresponds to the weak, very broad band at about 580 nm in the experimental spectra.§¶ The second band appears instead much more complex. It is contributed by a large number of lines on which the oscillator strength redistributes in different ways depending on the nature of the L ligand. In particular, a shoulder appears at the high energy side of this band in the spectrum of **4**, which becomes more pronounced for the pyridine compound (**8**) and extends the energy range of the band towards the UV spectral region. It is also apparent from the figure that the most intense transitions

§ It has to be noted that at this level of approximation the energy separation between the calculated bands can be taken with more confidence compared to calculated absolute excitation energies.

¶ The experimental low energy transition might be affected by strong vibrational broadening, which is not taken into account at all in the calculated spectra.

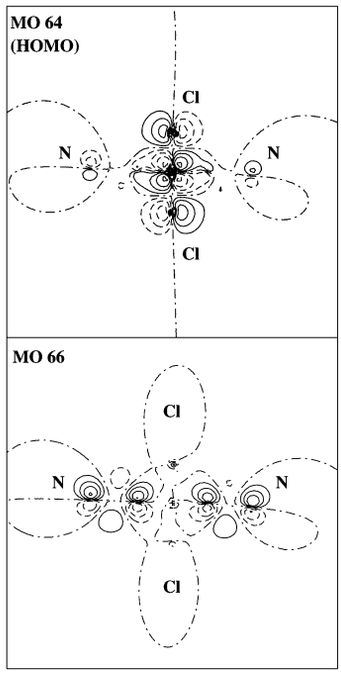

Fig. 8 Contour plots relative to selected initial and final MOs of *trans*,*trans*,*trans*-$ReO(OEt)Cl_2(pyz)_2$ **3**: solid, dashed and dot-dashed lines mean positive, negative and zero (nodal line) contribution respectively. Framework size: 20 au. The plots are referred to the planes containing the Cl atoms as well as the two N atoms of the pyz ligands.

that contribute to this band (**b**, **c**, and **d**, Fig. 7) shift slightly towards higher energies on going from the pyrazine to the pyridine compound. This behaviour mimics the trend observed experimentally for the relatively intense absorption band in the blue region of the spectrum.§

Owing to the complexity of this energy region it is useful to rationalize the calculated results on the basis of the nature of the initial and final states involved in the main transitions contributing to the two bands. For this purpose we analyse here in detail the spectrum of the pyrazine complex **3**, which represents an extreme term of the series. The assignment of the spectral features is guided by an inspection of the contour plots relative to the initial and final MOs involved in the main calculated transitions. It has to be noted that in all cases the contour plots of the wavefunctions are consistent with the Mulliken population analysis.

The low energy line **a** (Fig. 7) was attributed to the HOMO (MO 64) $\longrightarrow$ MO 66 transition. The contour plots corresponding to these orbitals (Fig. 8) indicate that the initial state (HOMO) is mainly associated to the rhenium 5d atomic orbital which interacts with the chlorine 3p orbitals to give rise to an essentially π^* molecular orbital. The final state (MO 66) is instead a pyz ligand molecular orbital in which contribution from the nitrogen 2p orbitals is well visible in the contour plot. Therefore the low energy spectral band can be ascribed to a transition from the rhenium 5d to an unoccupied diaza ligand MO. The nature of this transition has been verified also in the other two rhenium complexes and can therefore be considered responsible for the constant energy position and intensity calculated along the series.

Several higher energy transitions give rise to the second band in the spectrum; the three lines (**b**, **c**, and **d** in Fig. 7) which give the main contributions to the intensity of the band correspond to the MO 60 $\longrightarrow$ MO 67, MO 59 $\longrightarrow$ MO 67, and MO 57 $\longrightarrow$ MO 66 transitions, respectively. According to the contour plots (see ESI), lines **b** and **c** are ascribed to transitions from MOs with an essentially Cl ligand character towards a final state with predominant rhenium 5d contribution with an additional oxygen 2p participation. These transitions can be identified as charge transfer (CT) transitions from the ligand to

the metal orbitals. Interestingly, a reverse nature is instead found for line **d**, which involves an initial state with rhenium 5d and chlorine 3p mixed character and a final state with mainly pyz ligand contribution. A similar nature characterizes also the main transitions which contribute to the second band of the calculated spectrum of **4**, although a shift towards higher energy is observed for the third main line (**d**), as already commented. In the spectrum of the py complex (**8**) the energy order of these three transitions changes (Fig. 7) and a further increase of their excitation energies and intensities is observed. In particular, the main intensity contribution is now associated to a line (**e**, Fig. 7) which is again ascribed to a transition from a ligand orbital (with an essentially oxygen 2p participation) to a mainly rhenium 5d final state.

Reactivity of coordinated pyz and pym ligands

The compounds described above bear complexed bridging ligands and thus can be considered as basic building blocks; for example, *trans*,*trans*,*trans*-$ReO(OEt)Cl_2(pyz)_2$ **3** and [*trans*-$ReO_2(pyz)_4][PF_6]$ **7** are a linear and a cruciform building block, respectively.

For the time being, we investigated the reactivity of *trans*,*trans*,*trans*-$ReO(OEt)Cl_2(pyz)_2$ **3** (and of *trans*,*trans*,*trans*-$ReO(OEt)Cl_2(pym)_2$ **4**) towards metal centers which might belong either to a coordination complex or to a metalloporphyrin. As an example of coordination complex we used *cis*,*fac*-$RuCl_2(Me_2SO)_3(CO)$ **9**; we previously showed that treatment of **9** with heterocyclic N-donor ligands (L) leads to selective coordination of [*cis,cis,cis*-$RuCl_2(Me_2SO\text{-}S)_2(CO)$] fragments ([**Ru**]) to the nitrogen atoms.[19–21]

Treatment of *trans*,*trans*,*trans*-$ReO(OEt)Cl_2(pyz)_2$ **3** with a slight excess of **9** at ambient temperature (see ESI) led to the isolation in relatively good yield of the linear trinuclear compound [{*trans*,*trans*,*trans*-$ReO(OEt)Cl_2$}(μ-pyz)$_2${*cis*,*cis*,*cis*-$RuCl_2(Me_2SO\text{-}S)_2(CO)$}$_2$] **10**, which was characterized by elemental analysis, IR and ^{1}H NMR spectroscopy. The solid state IR spectrum of **10** lacked the characteristic sharp band for terminal pyrazine, suggesting its exclusively bridging coordination; moreover, it indicated the presence of carbonyl ligands, of exclusively S-bonded Me_2SO ligands, and of the Re=O and Re–OEt moieties. The ^{1}H NMR spectrum was rather straightforward: integration of the signals established the stoichiometry of the product (*i.e.* two [**Ru**] units per Re atom) and the number of resonances indicated that the two [**Ru**] units are equivalent. Coordination of the complexed pyz ligands of **3** to [**Ru**] affected mainly the resonances of the protons close to the previously unbound N atom (H3,5, $\Delta\delta = 0.42$); for comparison, coordination of pyz to [**Ru**] in the reference compound *cis*,*cis*,*cis*-$RuCl_2(Me_2SO\text{-}S)_2(CO)$(pyz) ([**Ru**](pyz), **11**) induced a $\Delta\delta = 0.46$ for the same protons. The four equally intense singlets in the region of S-bonded Me_2SO are consistent with the *cis*,*cis*,*cis* geometry for each [**Ru**] unit.‖

As an example of a metalloporphyrin we used [Ru(TPP)(CO)(EtOH)] (TPP = tetraphenylporphyrinate), which has a substitutionally labile axial ligand. Dinuclear compounds, consisting of two face-to-face ruthenium porphyrins linked together by axially bound pyrazine, 4,4′-bipy and similar ligands were reported in the past.[22] Very recently, an example in which the two porphyrins are axially connected through a bis(terpyridine) coordination compound has been described.[23]

Reaction of **3** with [Ru(TPP)(CO)(EtOH)], monitored by ^{1}H NMR spectroscopy ($CDCl_3$, ambient temperature), was quantitative and selective. Addition of one equivalent of [Ru(TPP)(CO)(EtOH)] to a $CDCl_3$ solution of **3** led readily (a few minutes) to the formation of two new species. Chemical shift considerations supported by integration and H–H COSY spectra allowed us to identify unambiguously the products as the unsymmetrical dinuclear compound [{*trans*,*trans*,*trans*-$ReO(OEt)Cl_2(pyz)$}(μ-pyz){Ru(TPP)(CO)}] **12**, in which the ruthenium porphyrin is bound only to one end of the rhenium complex, and the symmetrical trinuclear species [{*trans*,*trans*,*trans*-$ReO(OEt)Cl_2$}(μ-pyz)$_2${Ru(TPP)(CO)}$_2$] **13** (Fig. 9). Further addition of the ruthenium porphyrin led to the disappearence of the resonances of **12** and of residual **3** and to quantitative formation of **13**; all resonances are sharp, indicating that no significative dissociation of Ru(TPP)(CO) (**Ru**) from the adducts occurs in the millimolar range of concentrations. As in similar compounds, the shielding effect of the orthogonal (**Ru**) units decreases gradually as the (**Ru**)–proton distance increases.[21–24] Accordingly, in the dinuclear compound **12** the resonances of the protons on the pyz ring bound to (**Ru**) are dramatically shifted upfield, especially that of H3,5, while those of the protons on the pyrazine terminally bound to Re are only marginally affected. The resonances of the ethoxide protons, which are equally distant from the two termini of the rhenium complex, are shifted upfield equally by each (**Ru**) unit.

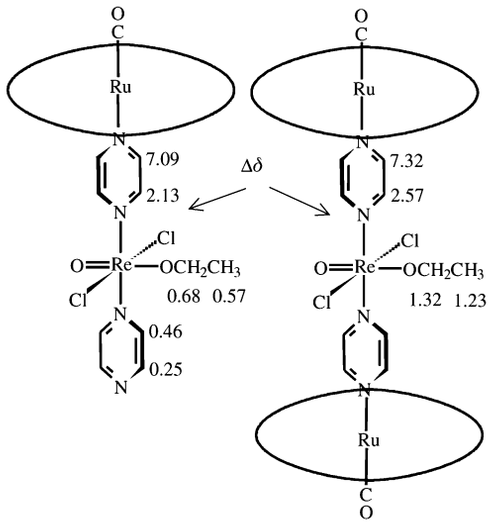

Fig. 9 Schematic drawings of [{*trans*,*trans*,*trans*-$ReO(OEt)Cl_2(pyz)$}(μ-pyz){Ru(TPP)(CO)}] **12** and [{*trans*,*trans*,*trans*-$ReO(OEt)Cl_2$}(μ-pyz)$_2${Ru(TPP)(CO)}$_2$] **13**; TPP is represented with an ellipse. Selected complexation induced shifts are marked on **12** and **13**, in ppm upfield relative to **3**.

Similarly, titration of [Ru(TPP)(CO)(EtOH)] into a $CDCl_3$ solution of *trans*,*trans*,*trans*-$ReO(OEt)Cl_2(pym)_2$ **4** led to the corresponding canted dinuclear and trinuclear compounds, [{*trans*,*trans*,*trans*-$ReO(OEt)Cl_2(pym)$}(μ-pym){Ru(TPP)(CO)}] **14** and [{*trans*,*trans*,*trans*-$ReO(OEt)Cl_2$}(μ-pym)$_2${Ru(TPP)(CO)}$_2$] **15**, respectively (see ESI).

Conclusion

We described here the synthesis and characterization of some new oxo- and dioxo-rhenium(v) species, both mononuclear and dinuclear, which bear one or more terminally coordinated pyrazine (pyz) or pyrimidine (pym) ligands. Most of them were prepared in good yield from the same oxorhenium(v) precursor, $ReOCl_3(Me_2S)(OPPh_3)$, by changing the reaction conditions. The new compounds were characterized in solution and in the solid state by spectroscopic techniques and the crystal structures of four of them, namely $Re_2O_3Cl_4(pyz)_4$ **1**, *trans*,*trans*,*trans*-$ReO(OEt)Cl_2(pyz)_2$ **3**, *trans*,*trans*,*trans*-$ReO(OEt)Cl_2(pyz)(PPh_3)$ **5**, and [*trans*-$ReO_2(pyz)_4][PF_6]\cdot NaPF_6\cdot 2H_2O$ **7**, were also determined. Density functional calculations of the electronic absorption spectra were performed for **3** and *trans*,*trans*,*trans*-$ReO(OEt)Cl_2(pym)_2$ **4** (and for the already known pyridine analogue) with the aim of gaining some insight into the

‖ Since the [**Ru**] unit is chiral, **10** must exist as a mixture of stereoisomers (with *C* and *A* [**Ru**] moieties) with potentially different NMR signals; however, at the field used the ^{1}H NMR signals were not distinct for the diastereoisomers.

remarkable influence of the nature of the diaza ligand L on the color of the complexes. Overall, the analysis of the calculated results indicates that the experimental spectral change associated with the nature of the L ligand can not be explained as a single effect acting along the series but rather as a concurrence of many contributions only partially common to the different compounds.

Compounds **1**–**4** and **7**, which bear more than one terminally bound diaza ligand, are particularly suited for the purpose of constructing multimetal supramolecular assemblies upon reaction of the unbound N atoms with other metal centers; for example, **3** and **7** can be considered as a linear and a cruciform basic building block, respectively. Indeed, the crystal structure of [*trans*-$ReO_2(pyz)_4$][PF_6]·$NaPF_6$·$2H_2O$ **7** showed that in the solid state the four pyrazine bases terminally bound to Re interact also with sodium ions, forming slightly distorted square cavities (side length *ca*. 7.4 Å), with Na and Re alternating in the corners. We also showed that the unbound termini of the diaza ligands in **3** and **4** are capable of further reaction with metal centers; treatment of **3** with a slight excess of the ruthenium(II) complex *cis*,*fac*-$RuCl_2(Me_2SO)_3(CO)$ **9** yields the linear trinuclear species [{*trans*,*trans*,*trans*-$ReO(OEt)Cl_2$}-(μ-pyz)$_2${*cis*,*cis*,*cis*-$RuCl_2(Me_2SO$-*S*$)_2(CO)$}$_2$] **10**, in which both ends of the linear rhenium complex are bound to a ruthenium coordination compound. Similarly, treatment of **3** with an excess of Ru(TPP)(CO)(EtOH) led to the symmetrical trinuclear species [{*trans*,*trans*,*trans*-$ReO(OEt)Cl_2$}(μ-pyz)$_2$-{Ru(TPP)(CO)}$_2$] **13**, consisting of two face-to-face ruthenium porphyrins axially connected through the rhenium coordination compound; the corresponding canted trinuclear species [{*trans*,*trans*,*trans*-$ReO(OEt)Cl_2$}(μ-pym)$_2${Ru(TPP)(CO)}$_2$] **15** was similarly obtained from **4**.

Experimental

Materials

Chemicals, including NH_4ReO_4 and deuteriated solvents, were purchased from Aldrich and used as received. Electronic absorption spectra were recorded in quartz cells with a JASCO UV/vis V500 spectrophotometer equipped with a Peltier thermostatic unit, Infrared spectra (KBr) on a Perkin-Elmer 2000 NIR FT-Raman spectrometer, ^{1}H and ^{31}P-{^{1}H} NMR spectra at 400 and 161.9 MHz, respectively, on a JEOL EX 400 FT spectrometer. NMR Spectra were recorded at room temperature, unless otherwise stated, with 4,4-dimethyl-4-silapentane-1-sulfonate (DSS) as an internal standard for D_2O solutions and residual non-deuteriated solvent signal as reference for DMSO-d_6 (δ 2.50), $CDCl_3$ (δ 7.26), and CD_2Cl_2 (δ 5.30) spectra.

Synthesis of the complexes

The complexes $ReOCl_3(Me_2S)(OPPh_3)$,[25] *cis*,*fac*-$RuCl_2(Me_2SO)_3(CO)$ **9**[19] and Ru(TPP)(CO)(EtOH)[26] were synthesized according to the reported procedures. $ReO(OEt)Cl_2(PPh_3)_2$ was prepared from NH_4ReO_4 with a procedure similar to that described by Johnson *et al*. for isomer **2**;[3] *trans*,*trans*,*trans*-$ReO(OEt)Cl_2(py)_2$ **8** was prepared by the method used for **3** and **4** (see below), with a py to Re ratio of 5 : 1.

$Re_2O_3Cl_4(pyz)_4$ 1. A solution of pyrazine (0.5 g, 6.25 mmol) in acetone (5 mL) was added dropwise to a stirred suspension of $ReOCl_3(Me_2S)(OPPh_3)$ (0.20 g, 0.30 mmol) in acetone (10 mL). The emerald-green solution obtained in a few minutes was concentrated to 5 mL and a few drops of diethyl ether were added. A deep green crystalline precipitate formed within a few hours, was collected by filtration, washed rapidly with water, cold acetone, and diethyl ether, and then vacuum dried (0.11 g, 78% based on Re). The complex contains 0.5 acetone molecule of crystallization (Found: C, 23.1; H, 1.99; N, 12.4. $C_{17.5}H_{19}Cl_4N_8O_{3.5}Re_2$ requires C, 23.0; H, 2.10; N, 12.3%); λ_{max}/nm (CH_2Cl_2) 385 (ε/dm^3 mol^{-1} cm^{-1} 5450), 455 (3650), 480 (3550) and 660 (br, 1850); ν_{max}/cm^{-1} 1593s (pyz breathing mode), 975m (Re=O), and 705s and 685s (Re–O–Re); δ_H (CD_2Cl_2) 8.31 (8H, m), 8.71 (8H, m).

$Re_2O_3Cl_4(pym)_4$ 2. The complex was prepared by the method used for **1**. A deep green crystalline precipitate formed in a few hours from the concentrated clear emerald-green solution. It was collected in 76% yield, washed and dried as above (Found: C, 22.9; H, 1.96; N, 12.4. $C_{17.5}H_{19}Cl_4N_8O_{3.5}Re_2$ requires C, 23.0; H, 2.10; N, 12.3%); λ_{max}/nm (CH_2Cl_2) 355 (sh, ε/dm^3 mol^{-1} cm^{-1} 7400) and 665 (br, 1650); ν_{max}/cm^{-1} 1595s (pym breathing mode), 976m (Re=O), and 707s and 678s (Re–O–Re); δ_H (CD_2Cl_2) 7.56 (4H, m, H5), 8.59 (4H, m, H4), 8.78 (8H, m, H2 + H6).

***trans*,*trans*,*trans*-$ReO(OEt)Cl_2(pyz)_2$ 3.** Pyrazine (0.7 g, 8.75 mmol) was added to a stirred suspension of $ReOCl_3(Me_2S)$-$(OPPh_3)$ (0.30 g, 0.45 mmol) in absolute ethanol (15 mL). The mixture was heated to reflux for 30 min, generating a clear brown-greenish solution. A dark purple-blue crystalline precipitate separated upon cooling and was removed by filtration, washed with cold ethanol and diethyl ether and vacuum dried (0.15 g, 70%) (Found: C, 24.9; H, 2.68; N, 11.5. $C_{10}H_{13}Cl_2N_4O_2Re$ requires C, 25.1; H, 2.74; N, 11.7%); λ_{max}/nm ($CHCl_3$) 415 (ε/dm^3 mol^{-1} cm^{-1} 7800) and 580 (vbr, 450); ν_{max}/cm^{-1} 1590m (pyz breathing mode), 962m (Re=O), and 920s (δ OCH_2); δ_H ($CDCl_3$) 1.06 (3H, t, ^3J 6.8, CH_3CH$_2$O), 3.82 (2H, q, ^3J 6.8 Hz, CH_3CH_2O), 8.78 (4H, m, H2,6), 8.95 (4H, m, H3,5).

***trans*,*trans*,*trans*-$ReO(OEt)Cl_2(pym)_2$ 4.** The complex was prepared by the method used for **3**. A light-violet microcrystalline precipitate separated from the clear blue solution upon cooling. It was separated in 80% yield (Found: C, 24.8; H, 2.65; N, 11.5. $C_{10}H_{13}Cl_2N_4O_2Re$ requires C, 25.1; H, 2.74; N, 11.7%); λ_{axm}/nm ($CHCl_3$) 386 (ε/dm^3 mol^{-1} cm^{-1} 6000) and 584 (vbr, 330); ν_{max}/cm^{-1} 1588s (pym breathing mode), 960m (Re=O), and 915s (δ OCH_2); δ_H ($CDCl_3$) 1.02 (3H, t, ^3J 7.2, CH_3CH$_2$O), 3.79 (2H, q, ^3J 7.2 Hz, CH_3CH_2O), 7.71 (2H, m, H5), 8.84 (2H, m, H4), 9.13 (2H, m, H6), 9.53 (2H, s, H2).

***trans*,*trans*,*trans*-$ReO(OEt)Cl_2(pyz)(PPh_3)$ 5.** Pyrazine (50 mg, 0.60 mmol) was added to a stirred suspension of ReO-$(OEt)Cl_2(PPh_3)_2$ (0.10 g, 0.12 mmol) in absolute ethanol (10 mL). The mixture was heated to reflux for 1.5 h, generating a clear brown-greenish solution. A dark purple-brown crystalline precipitate separated upon cooling; the product was removed by filtration after overnight standing at room temperature, washed with cold ethanol and diethyl ether and vacuum dried (35 mg, 45%) (Found: C, 43.8; H, 3.66; N, 4.28. $C_{24}H_{24}Cl_2N_2O_2PRe$ requires C, 43.6; H, 3.67; N, 4.24%); ν_{max}/cm^{-1} 1588s (pyz breathing mode), 949m (Re=O) and 916s (δ OCH_2); δ_H (selected, $CDCl_3$, −20 °C) 0.59 (3H, t, ^3J 6.0 Hz, CH_3CH$_2$O), 3.04 (2H, q, ^3J 6.0 Hz, CH_3CH_2O), 8.83 (2H, m, pyz), 8.91 (2H, m, pyz); δ_P ($CDCl_3$, external H_3PO_4) −5.54.

[*trans*-$ReO_2(pyz)_4$]Cl 6 and [*trans*-$ReO_2(pyz)_4$][PF_6] 7. Pyrazine (2.46 g, 30.8 mmol) was added to a stirred suspension of $ReOCl_3(Me_2S)(OPPh_3)$ (0.20 g, 0.30 mmol) in methanol–water (90 : 10, 30 mL). The mixture was heated to reflux for 2 h, yielding a clear deep orange solution. If the solution was allowed to cool to room temperature a yellow crystalline precipitate of **6** separated within a few hours and was removed by filtration, washed with cold methanol and diethyl ether, and vacuum dried (100 mg, 45%). According to elemental analysis the product contains four molecules of HCl of crystallization and is therefore better formulated as [*trans*-$ReO_2(pyz)_4$]Cl·4HCl (Found: C, 27.3; H, 2.86; N, 15.8. $C_{16}H_{20}Cl_5N_8O_2Re$ requires C,

Table 1 Crystal data and details of structure refinements for compounds $Re_2O_3Cl_4(pyz)_4$ **1**, *trans*,*trans*,*trans*-$ReO(OEt)Cl_2(pyz)_2$ **3**, *trans*,*trans*,*trans*-$ReO(OEt)Cl_2(pyz)(PPh_3)$ **5**, and [*trans*-$ReO_2(pyz)_4$][PF_6]·$NaPF_6$·$2H_2O$ **7**

	1·$0.5C_3H_6O$	**3**	**5**	**7**·$2H_2O$
Formula	$C_{17.5}H_{19}Cl_4N_8O_{3.5}Re_2$	$C_{10}H_{13}Cl_2N_4O_2Re$	$C_{24}H_{24}Cl_2N_2O_2PRe$	$C_{16}H_{20}F_{12}N_8NaO_4P_2Re$
Formula weight	911.61	478.34	660.52	887.53
Crystal system	Triclinic	Monoclinic	Monoclinic	Monoclinic
Space group	$P\bar{1}$	$P2_1/n$	$C2/c$	$P2/n$
a/Å	9.399(1)	11.804(3)	17.443(4)	9.243(1)
b/Å	10.244(2)	9.061(3)	8.891(1)	14.793(2)
c/Å	15.691(3)	14.253(4)	32.297(7)	10.560(1)
α/°	105.41			
β/°	96.36(1)	105.67(2)	97.80(2)	95.94(2)
γ/°	100.50(1)			
V/Å^3	1611.6(6)	1467.8(7)	4963(2)	1436.1(3)
Z	2	4	8	2
μ(Mo-Kα)/mm^{-1}	8.981	8.645	5.201	4.476
Reflections collected	6348	3574	6440	4539
Reflections unique (R_{int})	6118 (0.0214)	3340 (0.0726)	5953 (0.0550)	4187 (0.0481)
$R1$, $wR2$ ($I > 2\sigma(I)$)	0.0493, 0.1429	0.0691, 0.1823	0.0347, 0.1115	0.0396, 0.0955

26.7; H, 2.81; N, 15.6%); ν_{max}/cm^{-1} 1594m (pyz breathing mode) and 817m (O=Re=O); δ_H (D_2O) 8.77 (8H, m), 9.11 (8H, m).

Compound **7** was obtained by dropwise addition of a methanol solution (3 mL) of $NaPF_6$ (103.4 mg, 0.6 mmol) to the above warm solution. A yellow microcrystalline precipitate formed immediately and was removed by filtration, washed with cold methanol and diethyl ether, and vacuum dried. Slow evaporation of the mother liquor at ambient temperature yielded crystals of **7** suitable for X-ray analysis. According to elemental analysis the product contains one $NaPF_6$ and two H_2O molecules of crystallization and is therefore better formulated as [*trans*-$ReO_2(pyz)_4$][PF_6]·$NaPF_6$·$2H_2O$ (total 200 mg, 75%) (Found: C, 21.4; H, 2.24; N, 12.8. $C_{16}H_{20}F_{12}N_8NaO_4P_2Re$ requires C, 21.6; H, 2.27; N, 12.6%); ν_{max}/cm^{-1} 1595m (pyz breathing mode) and 810s (O=Re=O); δ_H (D_2O) 8.77 (8H, m), 9.11 (8H, m).

[{*trans*,*trans*,*trans*-ReO(OEt)Cl$_2$}(μ-pyz)$_2${*cis*,*cis*,*cis*-RuCl$_2$-(Me$_2$SO-*S*)$_2$(CO)}$_2$] 10. *trans*,*trans*,*trans*-$ReO(OEt)Cl_2(pyz)_2$ **3** (70 g, 0.14 mmol) was added to a chloroform solution (10 mL) of *cis*,*fac*-$RuCl_2(Me_2SO)_3(CO)$ **9** (160 mg, 0.36 mmol). The mixture was allowed to react at ambient temperature for 24 h and then vacuum evaporated to 3 mL and some diethyl ether added. The greenish brown precipitate which formed within 48 h was collected by filtration, washed with cold chloroform and diethyl ether, and vacuum dried (64 mg, 50%) (Found: C, 20.2; H, 3.17; N, 4.6. $C_{20}H_{37}Cl_6N_4O_8ReRu_2S_4$ requires C, 20.1; H, 3.13; N, 4.7%); ν_{max}/cm^{-1} 2009s (C≡O), 1119s (Me$_2$SO-*S*), 954m (Re=O), 918s (δ OCH_2) and 427m (Ru–S); δ_H ($CDCl_3$) 1.09 (3H, t, ^3J 7.2, CH_3CH_2O), 3.52, 3.54, 3.56, 3.59 (6H each, s, Me$_2$SO-*S*), 3.85 (2H, q, ^3J 7.2 Hz, CH_3CH_2O), 8.73 (4H, m, H2,6), 9.37 (4H, m, H3,5); δ_H (DMSO-d_6) 1.08 (3H, t, CH_3CH_2O), 3.42, 3.47, 3.55, 3.61 (6H each, s, Me$_2$SO-*S*), 3.87 (2H, q, CH_3CH_2O), 8.75 (4H, m, H2,6), 9.46 (4H, m, H3,5).

***cis*,*cis*,*cis*-RuCl$_2$(Me$_2$SO-*S*)$_2$(CO)(pyz) 11.** Pyrazine (74 mg, 0.92 mmol) was added to a solution of *cis*,*fac*-$RuCl_2(Me_2SO)_3(CO)$ **9** (0.20 g, 0.46 mmol) in chloroform (20 mL) and the system allowed to react overnight at ambient temperature. The orange solution was then concentrated to *ca*. 5 mL, 0.5 mL of diethyl ether added and stored at 4 °C. The product precipitated as orange-yellow microcrystals within a few days and was collected by filtration, washed with cold methanol and diethyl ether and vacuum dried (160 mg, 80%) (Found: C, 24.4; H, 3.68; N, 6.2. $C_9H_{16}Cl_2N_2O_3RuS_2$ requires C, 24.8; H, 3.69; N, 6.4%); ν_{max}/cm^{-1} 1592s (pyz breathing mode), 1976s (C≡O), 1094s (Me$_2$SO-*S*), 427m (Ru–S); δ_H ($CDCl_3$) 3.46, 3.51, 3.52, 3.57 (3H each, s, Me$_2$SO-*S*), 8.66 (2H, m, H3,5), 9.05 (2H, m, H2,6).

[{*trans*,*trans*,*trans*-ReO(OEt)Cl$_2$(pyz)}(μ-pyz){Ru(TPP)-(CO)}] 12, [{*trans*,*trans*,*trans*-ReO(OEt)Cl$_2$}(μ-pyz)$_2${Ru(TPP)-(CO)}$_2$] 13, [{*trans*,*trans*,*trans*-ReO(OEt)Cl$_2$(pym)}(μ-pym)-{Ru(TPP)(CO)}] 14, and [{*trans*,*trans*,*trans*-ReO(OEt)Cl$_2$}-(μ-pym)$_2${Ru(TPP)(CO)}$_2$] 15. All reactions between *trans*,*trans*,*trans*-$ReO(OEt)Cl_2(pyz)_2$ **3**, or *trans*,*trans*,*trans*-$ReO(OEt)Cl_2(pym)_2$ **4** and [Ru(TPP)(CO)(EtOH)] leading to compounds **12**–**15** were monitored by ^{1}H NMR spectroscopy in deuteriated chloroform at ambient temperature. The reactions were relatively fast (a few minutes at ambient temperature), quantitative (by NMR criteria) and very selective. Purple precipitates of the products formed in the NMR tube upon standing; the products however decomposed when purification by column chromatography on silica gel was attempted.

12: δ_H (selected, $CDCl_3$) 0.49 (3H, t, ^3J 8.0, OCH_2CH_3), 1.86 (2H, m, H3,5 bridge), 3.14 (2H, q, ^3J 8.0 Hz, OCH_2CH_3), 6.65 (2H, m, H2,6 bridge), 8.19 (8H, m, *o*H TPP), 8.32 (2H, m, H2,6 terminal), 8.70 (8H, s, βH TPP + 2H, m, H3,5 terminal).

13: δ_H (selected, $CDCl_3$) −0.17 (3H, t, ^3J 8.0, OCH_2CH_3), 1.63 (4H, d, ^3J 4, H3,5 bridge), 2.50 (2H, q, ^3J 8.0, OCH_2CH_3), 6.21 (4H, d, ^3J 4 Hz, H2,6 bridge), 8.01 (8H, m, *o*H TPP), 8.09 (8H, m, *o*H TPP), 8.58 (16H, s, βH TPP).

14: δ_H (selected, $CDCl_3$) 0.36 (3H, t, ^3J 7, OCH_2CH_3), 1.71 (1H, m, H4 bridge), 2.81 (2H, q, ^3J 7 Hz, OCH_2CH_3), 2.90 (1H, s, H2 bridge), 5.64 (1H, m, H5 bridge), 8.69 (8H, s, βH TPP), 8.75 (1H, m, H6 terminal), 8.75 (1H, m, H4 terminal), 9.19 (1H, s, H2 terminal). The resonances of H5 terminal and H6 bridge overlap with the signals of the phenyl rings.

15: δ_H (selected, $CDCl_3$) −0.42 (3H, t, ^3J 7 Hz, OCH_2CH_3), 1.61 (2H, m, H4 bridge), 2.00 (2H, q, ^3J 7 Hz, OCH_2CH_3), 2.47 (2H, s, H2 bridge), 5.57 (2H, m, H5 bridge), 8.59 (16H, s, βH TPP). The resonance of the H6 bridge overlaps with the signals of the phenyl rings.

X-Ray diffraction

Crystal parameters and details of the structure determination for compounds **1**, **3**, **5** and **7** are summarized in Table 1. The data sets for **1**, **5** and **7** were collected on a Enraf-Nonius CAD4 diffractometer, that for **3** on a Kuma KM4 instrument; both were equipped with a graphite monochromator and Mo-Kα radiation (λ = 0.71073 Å). The measurements were carried out at room temperature (273(2) K) using the ω–2θ scan technique. Three standard reflections, measured at regular intervals, showed no significant variation in intensity in all the data collections. The reflections were corrected for Lorentz-polarization effects and for absorption, based on an empirical ψ-scan method. All the structures were solved by Patterson and Fourier analyses[27] and refined by the full-matrix least-squares method based on F^2 with all observed reflections.[28]

A molecule of acetone with occupancy of 0.5 (on the basis of the electron density peaks) was detected in the ΔF map of **1**. The final cycles with fixed contribution of hydrogen atoms, (excluding those of the acetone molecule in **1**) converged to final $R1$ and $wR2$ factors reported in Table 1. All the calculations were performed using the WinGX System, Version 1.61.[29]

CCDC numbers 153388–153391.

See http://www.rsc.org/suppdata/dt/b0/b009295i/ for crystallographic data in CIF or other electric format.

Computational model

The electronic structure of the *trans*,*trans*,*trans*-ReO(OEt)-$Cl_2(L)_2$ complexes (L = pyz (**3**), pym (**4**) or py (**8**)) was obtained by solving the Kohn–Sham (KS) equations, in the framework of the Density Functional Theory (DFT), employing the ADF program.[30,31] During the Self Consistent Field (SCF) procedure the local density approximation (LDA) to the exchange correlation energy functional was self-consistently employed, based on the Vosko, Wilk and Nusair (VWN) parametrization.[32]

A frozen core Double Zeta plus Polarization Slater Type Orbitals (DZP STO) basis set was used for the non-transition atoms, while for the rhenium atom a Triple Zeta (TZ) set was chosen. All basis sets were taken from the ADF database. In a previous study on transition metal complexes this choice proved to be a good compromise between accuracy and computational effort.[33]

The excitation energies were calculated as differences between the KS eigenvalues of unoccupied and occupied molecular orbitals (MO). In order to have a quantitative description of the excitation spectrum, the transition probabilities among all the occupied MOs and the first seven low-lying unoccupied MOs were evaluated. To this purpose we employed a previous implementation of the ADF code for the calculation of dipole integrals.[34] The oscillator strength f is the absolute measure of the transition intensity and it defined as $f_{if} = \frac{2}{3}\omega_{if} n_i |\langle\varphi_i|\vec{r}|\varphi_f\rangle|^2$ where $\omega_{if} = \varepsilon_f - \varepsilon_i$, ε is the KS eigenvalue, ω the excitation energy, n_i the occupation number of the initial state, φ_i, φ_f are the initial and final MOs, respectively, and $\vec{r}$ is the dipole operator. The excitation spectrum is obtained in terms of the calculated intensity (oscillator strength f) as a function of the excitation energy and can therefore be directly compared with the experimental measure.

Experimental geometries were used for compound **3** (present work) and **8** (ref. 6). X-Ray investigation of low-quality crystals of the pym compound **4** allowed us to establish that also in this case the two *trans* bases are coplanar. Thus, the same geometrical parameters as for **3** were used, exchanging the coordinates of the atoms at positions 3 and 4. Calculations were performed for both *cis* and *trans* conformers, giving no appreciably different results.

Acknowledgements

We thank the Italian MURST for financial support and F. Princivalle (Dipartimento Scienze della Terra, University of Trieste) who collected X-ray data for **3**. This work was performed in the framework of EU program COST Action D11, project no. D11/0004/98.

References

1 J.-L. Lehn, *Supramolecular Chemistry: concepts and perspectives*, VCH, Weinheim, 1995; M. Fujita, *Chem. Soc. Rev.*, 1998, **27**, 417; S. Leininger, B. Olenyuk and P. J. Stang, *Chem. Rev.*, 2000, **100**, 853; G. F. Swiegers and T. J. Malefetse, *Chem. Rev.*, 2000, **100**, 3483.
2 E. C. Constable and A. M. W. Cargill Thompson, *J. Chem. Soc.*, *Dalton Trans.*, 1994, 1409; R. V. Slone, D. Y. Yoon, R. M. Calhoun and J. T. Hupp, *J. Am. Chem. Soc.*, 1995, **117**, 11813; K. Wärnmark, J. A. Thomas, O. Heyke and J.-M. Lehn, *Chem. Commun.*, 1996, 701; J. A. Whiteford, C. V. Lu and P. J. Stang, *J. Am. Chem. Soc.*, 1997, **119**, 2524; J. Manna, C. J. Kuehl, J. A. Whiteford, P. J. Stang, D. C. Muddiman, S. A. Hofstadler and R. D. Smith, *J. Am. Chem. Soc.*, 1997, **119**, 11611; P. J. Stang and N. E. Persky, *Chem. Commun.*, 1997, 77; C. Müller, J. A. Whiteford and P. J. Stang, *J. Am. Chem. Soc.*, 1998, **120**, 9827; T. Kajiwara and T. Ito, *J. Chem. Soc.*, *Dalton Trans.*, 1998, 3351; A. Mayr and J. Guo, *Inorg. Chem.*, 1999, **38**, 921; R.-D. Schnebeck, E. Freisinger and B. Lippert, *Chem. Commun.*, 1999, 675; K. Chichak and N. R. Branda, *Chem. Commun.*, 2000, 1211; S.-S. Sun, A. S. Silva, I. M. Brinn and A. J. Lees, *Inorg. Chem.*, 2000, **39**, 1344; E. Iengo, B. Milani, E. Zangrando, S. Geremia and E. Alessio, *Angew. Chem.*, *Int. Ed.*, 2000, **39**, 1096.
3 N. P. Johnson, C. J. L. Lock and G. Wilkinson, *J. Chem. Soc.*, 1964, 1054.
4 N. P. Johnson, F. I. M. Taha and G. Wilkinson, *J. Chem. Soc.*, 1964, 2614.
5 C. J. L. Lock and G. Turner, *Can. J. Chem.*, 1978, **56**, 179.
6 C. J. L. Lock and G. Turner, *Can. J. Chem.*, 1977, **55**, 333.
7 C. J. L. Lock and G. Turner, *Acta Crystallogr.*, *Sect. B*, 1978, **34**, 923; J. M. Botha, A. Roodt and J. G. Leipoldt, *S. Afr. J. Chem.*, 1995, **48**, 120.
8 L. G. Marzilli, M. Iwamoto, E. Alessio, L. Hansen and M. Calligaris, *J. Am. Chem. Soc.*, 1994, **116**, 815; E. Alessio, L. Hansen, M. Iwamoto and L. G. Marzilli, *J. Am. Chem. Soc.*, 1996, **118**, 7593.
9 C. K. Johnson, ORTEP II, Report ORNL-5138, Oak Ridge National Laboratory, Oak Ridge, TN, 1976.
10 C. Pearson and A. L. Beuchamp, *Acta Crystallogr.*, *Sect. C*, 1994, **50**, 42.
11 S. Fortin and A. L. Beauchamp, *Inorg. Chim. Acta*, 1998, **279**, 159.
12 G. Backes-Dahmann and J. H. Enemark, *Inorg. Chem.*, 1987, **26**, 3960.
13 L. Hansen, E. Alessio, M. Iwamoto, P. A. Marzilli and L. G. Marzilli, *Inorg. Chim. Acta*, 1995, **240**, 413; E. Alessio, E. Zangrando, E. Iengo, M. Macchi, P. A. Marzilli and L. G. Marzilli, *Inorg. Chem.*, 2000, **39**, 294.
14 F. H. Allen, O. Kennard and R. Taylor, *Acc. Chem. Res.*, 1983, **16**, 146.
15 A. M. Lebuis and A. L. Beuchamp, *Acta Crystallogr.*, *Sect. C*, 1994, **50**, 882.
16 S. Belanger and A. L. Beauchamp, *Inorg. Chem.*, 1996, **35**, 7836.
17 J. P. Collman, J. T. McDevitt, C. R. Leinder, G. T. Yee, J. B. Torrance and W. A. Little, *J. Am. Chem. Soc.*, 1987, **109**, 4606.
18 G. F. Ciani, G. D'Alfonso, P. F. Romiti, A. Sironi and M. Freni, *Inorg. Chim. Acta*, 1983, **72**, 29.
19 E. Alessio, B. Milani, M. Bolle, G. Mestroni, P. Faleschini, F. Todone, S. Geremia and M. Calligaris, *Inorg. Chem.*, 1995, **34**, 4722.
20 E. Alessio, M. Macchi, S. L. Heath and L. G. Marzilli, *Inorg. Chem.*, 1997, **36**, 5614.
21 E. Alessio, E. Ciani, E. Iengo, V. Yu. Kukushkin and L. G. Marzilli, *Inorg. Chem.*, 2000, **39**, 1434.
22 V. Marvaud and J.-P. Launay, *Inorg. Chem.*, 1993, **32**, 1376; A. Endo, Y. Okamoto, K. Suzuki, J. Shimamura, K. Shimizu and G. P. Satô, *Chem. Lett.*, 1994, 1317; A. Endo, U. Tagami, Y. Wada, M. Saito, K. Shimizu and G. P. Satô, *Chem. Lett.*, 1996, 243.
23 K. Chichak and N. R. Branda, *Chem. Commun.*, 1999, 523.
24 E. Alessio, M. Macchi, S. Heath and L. G. Marzilli, *Chem. Commun.*, 1996, 1411.
25 D. E. Grove and G. Wilkinson, *J. Chem. Soc. A*, 1966, 1224; J. C. Bryan, R. E. Stenkamp, T. H. Tulip and J. M. Mayer, *Inorg. Chem.*, 1987, **26**, 2283; M. M. Abu-Omar and S. I. Khan, *Inorg. Chem.*, 1998, **37**, 4979.
26 J. J. Bonnet, S. S. Eaton, G. R. Eaton, R. H. Holm and J. A. Ibers, *J. Am. Chem. Soc.*, 1973, **95**, 2141.
27 G. M. Sheldrick, *Acta Crystallogr.*, *Sect. A*, 1990, **46**, 467.
28 G. M. Sheldrick, SHELXL 97, Program for crystal structure refinement, University of Göttingen, 1997.
29 L. J. Farrugia, *J. Appl. Crystallogr.*, 1999, **32**, 837.
30 E. J. Baerends, D. E. Ellis and P. Ros, *Chem. Phys.*, 1973, **2**, 41.
31 C. Fonseca Guerra, J. G. Snijders, G. te Velde and E. J. Baerends, *Theor. Chim. Acta.*, 1998, **99**, 391.
32 S. H. Vosko, L. Wilk and M. Nusair, *Can. J. Phys.*, 1980, **58**, 1200.
33 M. Stener and M. Calligaris, *J. Mol. Struct. (Theochem)*, 2000, **497**, 91.
34 M. Stener, A. Lisini and P. Decleva, *Chem. Phys.*, 1995, **191**, 141.